

# Investigations on Melting and Welding of Glass by Ultra-short Laser Radiation

Alexander HORN\*, Ilja MINGAREEV\* and Alexander WERTH\*

\*Lehrstuhl für Lasertechnik, Rheinisch-Westfälische Technische Hochschule Aachen,  
Steinbachstrasse 15, 52074 Aachen, Germany  
E-mail: alexander.horn@ilt.rwth-aachen.de

The interaction of laser radiation with pulse duration at 80 fs and wavelength  $\lambda = 800$  nm with BK7 glass is detected by pump&probe techniques. No melt ejection dynamics can be observed in the time-range of 100 ns to 1.6  $\mu$ s by irradiating with a single pulse a glass on the surface using time-resolved shadowgraphy. Using ultra-short pulsed laser radiation glass plates are welded together. The pump beam is focussed by a microscope objective ( $2\omega_0 \approx 4 \mu$ m) into the glass. After partial absorption of the optical energy the glass is heated. Due to the large intensities in the focus using high NA objectives multi-photon absorption gets the dominant process and due to large repetition rates heat is accumulated and melting of the glass is induced. By setting the intensity of the laser radiation below the ablation threshold glass can be melted inside and on the surface without cracking which makes welding of glass possible. The modification of a technical glass (D263 Schott) induced by ultra-short pulsed laser radiation with large repetition rates up to 1 MHz is observed during welding by time-resolved quantitative phase microscopy. The change in refractive index induced is detected.

**Keywords:** Pump&probe, welding, glass, ultrafast, refractive index

## 1. Introduction

Ultra-fast laser radiation is commonly used for precise micro structuring by ablation without affecting the bulk material with heat and thermo-mechanical stress. Due to ultra-fast pulse duration high-intensities are reachable at small fluences enabling multi-photon processes in dielectrics close to the ablation threshold. The observed processes are irreversible refractive index change, birefringence and electro-optical activity. The involved processes during irradiation are not completely understood, but some approaches are given. A non-thermal process starting from the generation of free electrons due to multi-photon absorption induces defects like short-living STE and long living NBOH and F-centers [1]. The density is changed by changing binding distances between Silicon and Oxygen atoms. On the other side a thermal process is possible by heating of the glass due to the relaxation of the electron system into the phonon system [2]. The glass is heated locally [4]; large compression forces within a very small volume change the density of the glass. Welding of glass has been achieved and also of silicon [5][6][7][8][9][10].

In this paper the interaction of ultra-fast laser radiation with glass is investigated firstly by observing the expansion of vapor and melt after irradiating the surface of BK7 glass with one pulse of laser radiation at 800 nm wavelength and 80 fs pulse duration. Secondly two glass plates are joined together by welding with femtosecond laser radiation and the welding zone is investigated dynamically by a new technique and also by analyzing the cross-section geometry of welding seams after irradiation.

## 2. Experimental Setup and diagnostics

### 2.1 Welding system

Plates of technical borosilicate display glass (SCHOTT D263) with thicknesses 1 mm and 200  $\mu$ m have been processed by RCA-cleaning and subsequently pressed together. Joining of glass is achieved by focusing high-repetition rate ultrafast laser radiation (IMRA  $\mu$ Jewel D-400,  $\lambda = 1045$ nm,  $t_p = 350$  fs) within two glass plates and moving the plates relative to the laser focus parallel to the interface between the plates. The laser radiation is guided by mirrors from the laser source to a positioning stage (KUGLER Microstep) and focused by a microscope objective to a diameter of 4  $\mu$ m (LEICA 20x, NA 0.4) between two glass plates (Fig. 1 and 2). Welding seams are generated moving the plates at a fixed velocity and focal position relative to the interface.

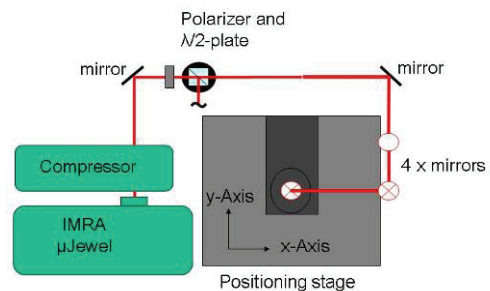


**Fig. 1** Welding setup.

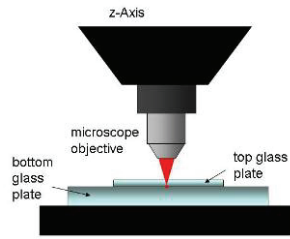


Fig. 2 Scheme of focusing microscope objective, top and bottom glass plate.

### 2.2 Single-Shot Quantitative Phase Microscopy

In order to detect mechanical stress induced by compression the refractive index is detected by quantitative phase microscopy (QPM) being proportional to the density change. QPM solves the intensity transport equation

$$k \frac{\partial I(\vec{r}_\perp)}{\partial z} = -\nabla_\perp \cdot (I(\vec{r}_\perp) \nabla_\perp \Phi(\vec{r}_\perp)) \quad (1)$$

of three object pictures taken by classical optical microscopy with Köhler illumination at different focal positions, e.g. focal, extra focal, and intra focal position. The resulting calculated quantitative phase distribution can be used for representation of the DIC, HMC, Darkfield or by calculating the refractive index when the investigated geometry is known. For the observation of dynamical processes, which are not reproducible, the three images have to be taken at the same time (Fig. 3). The light from an object is separated by beam splitter (BS) and the object at the three focal positions is imaged by lenses on a CCD (AVT Dolphin F145B).

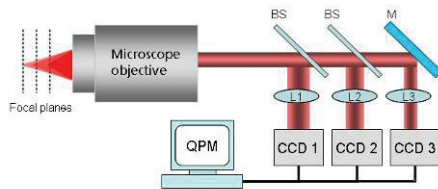


Fig. 3 Principle of Single-Shot Quantitative Phase microscopy.

The new concept - Single-Shot Quantitative Phase Microscopy (SS-QPM) - combines three CCD cameras with a commercial microscope (LEICA DML Fig. 4). Using custom-made software, images are acquired from the CCDs and pre-processed for QPM, thereafter the resulting phase is calculated.

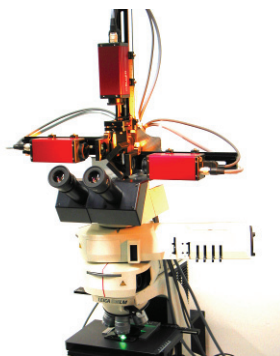


Fig. 4 Set-up of 3 CCD cameras on a commercial microscope.

### 2.3 SS-QPM of ablation and welding seam

The ablation of glass induced by single pulse femtosecond laser radiation ( $\lambda = 800 \text{ nm}$ ,  $t_p = 80 \text{ fs}$ ) has been investigated by pump&probe shadowgraphy up to  $1.6 \mu\text{s}$  delay between pump and probe pulse. The set-up used is described elsewhere [3].

The refractive index within the welding seam has been detected by combining SS-QPM, mounted on a microscope, with two laser sources (Fig. 5): The first one, IMRA  $\mu\text{Jewel D-400}$ , is used for welding as described in chapter 2.1. For illumination of the welding area a second laser source, THALES Concerto, is used at 0.5 Hz repetition rate. The dependence of the pump pulse (IMRA) to the illuminating probe pulse (CONCERTO) is detected by a photodiode. The laser systems are not temporally synchronized resulting in random delays between pump and probe. After measuring the data has to be re-sorted. The wavelength of the illuminating source can be changed between fundamental wavelength (800 nm), SHG (400 nm) and WLC (400-800nm).

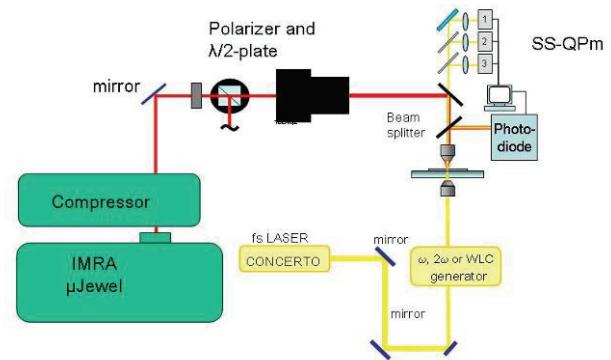


Fig. 5 Set-up for SS-QPM of welding seam.

The spatially integrated optical plasma emission observed during welding is continuous between 300 and 900 nm, with the maximum at about 550 nm and being small above 700 nm (OCEAN OPTICS USB2000 fiber spectrometer, Fig. 6). The optical plasma emission near the detection wavelength can be suppressed by edge filters, highly transmissive at  $> 750 \text{ nm}$ . The results on phase and refractive index measurements presented use the fundamental wavelength in order to suppress the optical emission from the plasma within the welding seam.

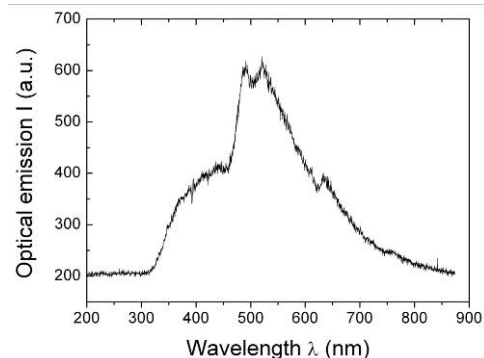


Fig. 6 Optical emission of plasma from the welding seam.

### 3. Results and discussion

#### 3.1 Morphology of welding seam

The welding seam has been detected by Nomarsky microscopy emphasizing two welding seam regions b1 and b2 (Fig. 7). The welding process is interrupted when contamination at the interface deflected the laser radiation and can be detected by interruptions of the welding seam.

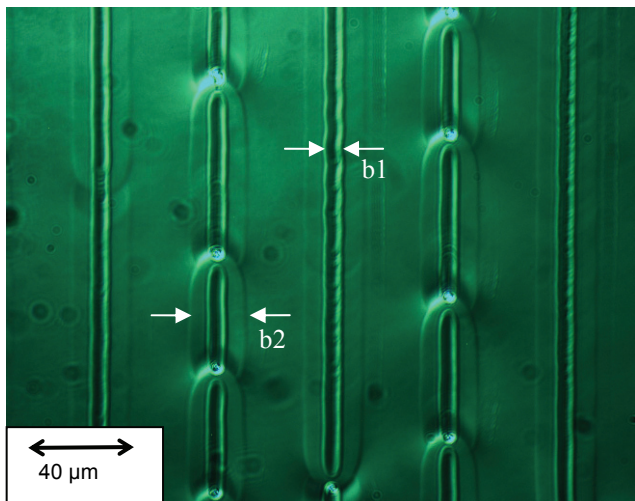


Fig. 7 Welding seams by Nomarsky microscopy .

Cross-sections of the welding seams have been made by cutting strips using UV nanosecond laser radiation and incorporating the welded substrates into a resin and thereupon lapping and polishing both sides up to optical surface quality (Fig. 8 and Fig. 9). The cross-sections are detected by Nomarsky microscopy exhibiting modifications in case of non-welding due to contaminations at the interface and an elliptical welding seam with the two regions (Fig. 8).

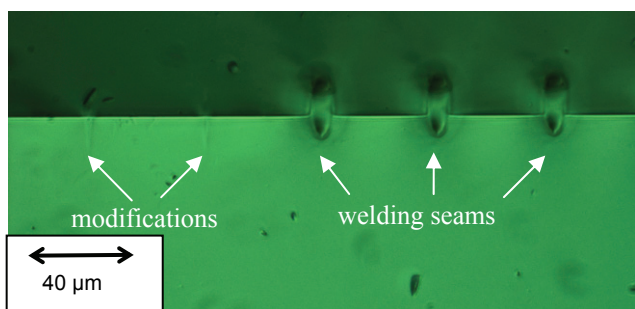


Fig. 8 Cross-section of 2 modifications (left) and 3 welding seams at the interface.

The welding seams at different welding positions  $z$  from the interface consist of a smaller region (width  $b_1$  and height  $h_1$ ) and a larger region (width  $b_2$  and height  $h_2$ ) (Fig. 9). The smaller region is characterized by two dark spots, one larger toward the incoming laser radiation. The welding by molten glass between the two glass plates can be observed within the small region, not in the larger region.

Measuring the widths and heights of the welding seams as function of the welding position results in an average welding height of about 30  $\mu\text{m}$ . Welding is achieved when

the welding seam has contact to the interface: no welding has been detected when the welding position  $z$  is larger than the welding height  $h_2$  (Fig. 10). With increasing welding position the widths increase slightly. This increase is more pronounced for the welding width  $b_2$  (Fig. 11). Contrary to other authors using different glass sorts and objective NA [11] welding was achieved only in the smaller region.

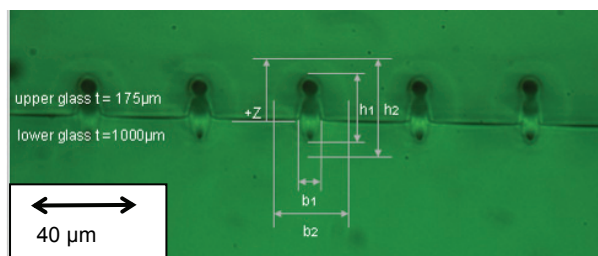


Fig. 9 Cross-section welding seams at the interface.

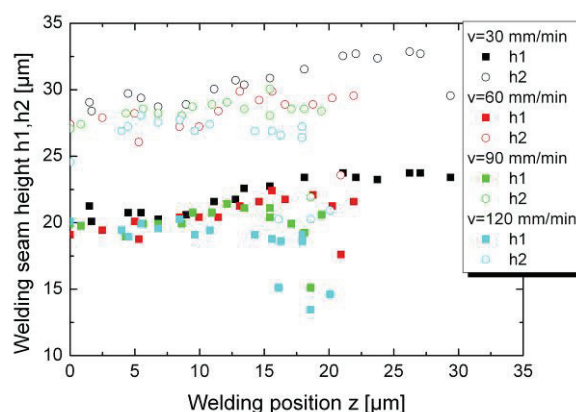


Fig. 10 Welding seam height  $h_1, h_2$  as function of welding position and velocity ( $E_p = 316 \text{ nJ}$ ).

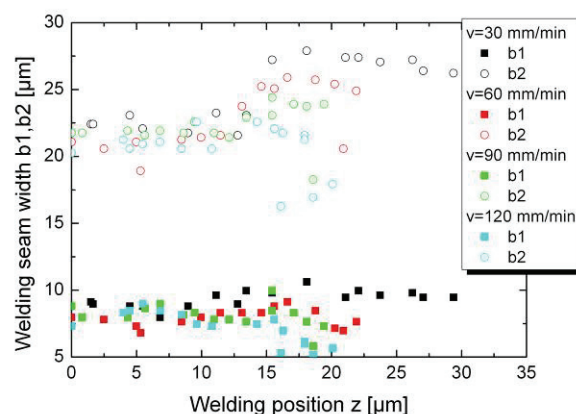
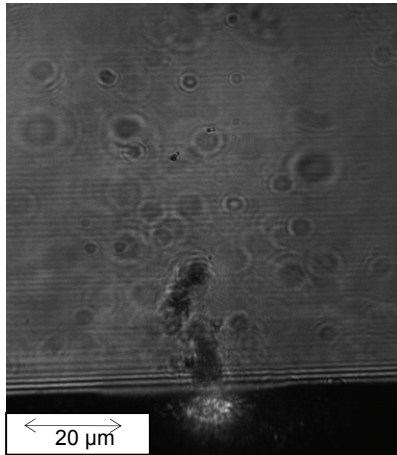


Fig. 11 Welding seam width  $b_1, b_2$  as function of welding position and velocity ( $E_p = 316 \text{ nJ}$ ).



### 3.2 Single pulse ablation of glass

Irradiating the surface BK7 glass by focusing single femtosecond laser pulses ( $I \approx 10^{13}$  W/cm<sup>2</sup>) generates by strong ablation dense plasma and after about 100 ns a strong emission of vapor and particles can be observed up to 1.6  $\mu$ s by shadowgraphy. But different to ablation of metals [3] no transient melt ejection can be observed (Fig. 12). Due to charge separation, coulomb explosion inhibits the formation of melt.



**Fig. 12** Vapor and particle emission after irradiation of BK7 glass with single femtosecond pulse ( $\lambda = 800$  nm,  $t_p = 80$  fs,  $E_p = 10$   $\mu$ J, delay 1.04  $\mu$ s).

### 3.3 Measurement of refractive index during welding

Using SS-QPm the refractive index distribution of the region around the welding seams has been measured after irradiation of D263 glass using incandescent white-light as illumination (Fig. 13 left).

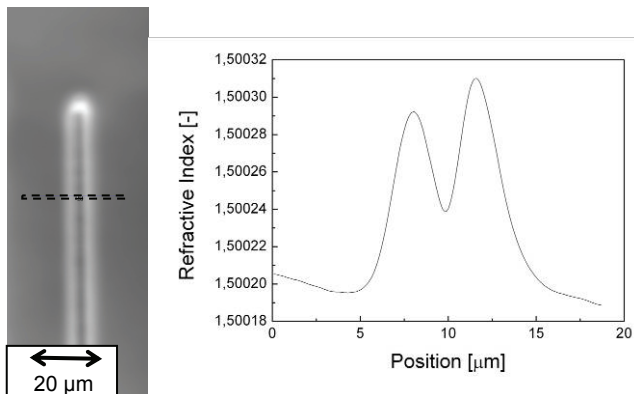


**Fig. 13** Refractive index distribution of welding seams and refractive index of cross-section.

The calculated refractive index distribution of the cross section of the welding seam results in two maxima at the borders and a relative minimum at the middle of the welding seam (Fig. 13 right). The refractive index is possibly reduced due to the melting and boiling within the laser interaction zone during the welding process.

### 3.4 Time dependence of refractive index during welding

Welding of D263 glass has been achieved at fixed welding seam position and the refractive index distribution has been measured by SS-QPm at welding velocity  $v = 60$  mm/min. The refractive index distribution for 4 delay times after pump pulse (IMRA) emphasizes a refractive index decrease within the laser interaction zone shortly after irradiation ( $t = 0$   $\mu$ s). This decrease can be attributed to the generation of free electrons. Nearby to the laser interaction zone an increase of refractive index is measured. With increasing delay up to  $t = 2.1$   $\mu$ s the refractive index within the interaction zone increases (Fig. 14).

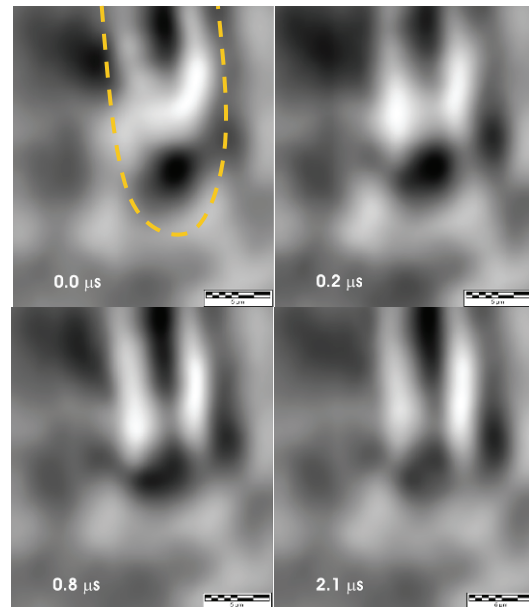


**Fig. 14** Refractive index distribution of welding zone for different delay times (contour of welding seam by dotted line).

## 4. Conclusion

Using ultra-fast laser radiation ( $t_p = 80$  fs,  $\lambda = 800$  nm) the ablation of glass (BK7) has been investigated. At large intensities above ablation threshold vapor and particles are emitted without continuous melt ejection.

Welding of two plates of technical borosilicate glass (D263) has been successfully performed by focused high-repetition ultra-fast laser radiation (IMRA  $\mu$ Jewel D-400,  $\lambda = 1045$  nm,  $t_p = 350$  fs). The geometry of welding seam has been investigated and the width, height and position relative to the interface have been detected for different values of welding velocity. An increase of the width for symmetric position relative to the welding zone has been detected. No welding has been detected when the welding position  $z$  is larger than the welding height. The refractive index distribution of a welding seam has been measured by quantitative phase microscopy (QPm). The refractive index is larger at the outer border than in the center of the welding seam. By a new technique, single-shot QPm, the dynamics of refractive index distribution of a welding seam has been measured. A strong decrease in refractive index during irradiation within the interaction zone has been observed.

### Acknowledgments and Appendixes

The authors would like to thank IMRA America for providing the  $\mu$ Jewel D-400 laser system within the framework "Premium Application Lab" (PAL).

### References

- [1] D. Wortmann, M. Ramme, J. Gottmann, "Volume waveguides by refractive index modification using fs-laser double pulses and ps-laser radiation ", Submitted to Proceedings of the 4th International Congress on Laser Advanced Materials Processing, May 2006, Kyoto, Japan
- [2] C. B. Schaffer, J. F. Garcia, E. Mazur: „Bulk heating of transparent materials using a high-repetition-rate femtosecond laser, Appl. Phys. A76, p.351 (2003)
- [3] I. Mingareev, A. Horn and E.W. Kreutz, Observation of melt ejection in metals up to 1  $\mu$ s after femtosecond laser irradiation by a novel pump-probe photography setup, Proc. of SPIE 6261, 62610A-1 (2006)
- [4] A. Horn I. Mingareev, I. Miyamoto, Ultra-fast diagnostics of laser-induced melting of matter, JLMN-Journal of Laser Micro/Nanoengineering Vol. 1, No. 3, 264-268 (2006)
- [5] I. Miyamoto, A. Horn, J. Gottmann, Local melting of glass material and its application to directfusion welding by ps-laser pulses, JLMN-Journal of Laser Micro/Nanoengineering Vol. 2, No. 1, 7-14 (2007)
- [6] I. Miyamoto, A. Horn, J. Gottmann, High-precision, high-throughput fusion welding of glass using femtosecond laser pulses, JLMN-Journal of Laser Micro/Nanoengineering Vol. 2, No. 1, 57-63 (2007)
- [7] T. Tamaki, W. Watanabe, J. Nishii, and K. Itoh, "Welding of transparent materials using femtosecond laser pulses," Jpn. J. Appl. Phys., Vol. 44, No. 22, L687-L689 (2005).
- [8] W. Watanabe, S. Onda, T. Tamaki, K. Itoh, and J. Nishii, "Space-selective laser joining of dissimilar transparent materials using femtosecond laser pulses," Appl. Phys. Lett., Vol. 89, No. 2, 021106 (2006).
- [9] T. Tamaki, W. Watanabe, and K. Itoh, "Laser micro-welding of transparent materials by a localized heat accumulation effect using a femtosecond fiber laser at 1558 nm," Opt. Express, Vol. 14, No. 22, 10460-10468 (2006).
- [10] W. Watanabe, S. Onda, T. Tamaki, and K. Itoh, "Direct joining of silica glass substrates by 1 kHz femtosecond laser pulses," Appl. Phys. B, vol. 87, pp. 85-89 (2007).
- [11] J. Bovatsek, A. Arai, C.B. Schaffer, "Three-Dimensional Micromachining Inside Transparent Materials Using Femtosecond Laser Pulses: New Applications", Submitted to CLEO/PhAST 2006 (2006).

(Received: May 14, 2007, Accepted: March 18, 2008)